Hindawi
Advances in Meteorology
Volume 2020, Article ID 2814539, 13 pages
https://doi.org/10.1155/2020/2814539

Research Article

Large-Scale Linkages of Socioeconomic Drought with Climate Variability and Its Evolution Characteristics in Northwest China

Siyuan Liu, Jianfeng Zhang, Ni Wang, and Na Wei

State Key Laboratory of Eco-hydraulics in Northwest Arid Region, Xi'an University of Technology, Xi'an 710048, China

Correspondence should be addressed to Jianfeng Zhang; jfzhang@mail.xaut.edu.cn

Received 24 October 2019; Revised 25 December 2019; Accepted 31 January 2020; Published 26 February 2020

Academic Editor: Pedro Salvador

Socioeconomic drought is one of the most frequent natural disasters in the world and is closely related to human life. The main cause of socioeconomic drought is the contradiction between water supply and demand; hence, as local reservoirs play a major role in improving water supply and coping with extreme climate, it is reasonable to estimate socioeconomic drought based on reservoir operations. The multivariate standardized reliability and resilience index (MSRRI) is utilized to evaluate socioeconomic drought, considering the characteristics of reservoir management and storage water resources. Therefore, with the MSRRI, this study takes the Heihe River Basin in northwestern China, which is controlled by two reservoirs dominating the upstream and downstream regions, as a case study to reveal the evolution characteristics of socioeconomic drought in the basin and the external impacts of climate variability. The results showed that (1) the drought intensity in the up-midstream region is stronger than that in the downstream region; in view of the hysteresis in the downstream region, the occurrence of drought in the up-midstream region could be regarded as an early warning to implement preventive measures in the downstream region; (2) an increasing trend in socioeconomic drought throughout the basin exists on both monthly and annual scales, which indicates that the increasing possibility of drought should be effectively addressed; (3) cross wavelet analysis indicated that the large-scale climate indices contribute to the variations in the socioeconomic droughts throughout the basin, indicating that climate variability may provide a reference for managers to deal with socioeconomic drought in the HRB.

1. Introduction

As one of the natural disasters most closely related to human life, droughts occur in almost all areas of the world and cause an average of $6~8 billion global damage annually [1, 2]. Drought places large demands on water resources in urban and rural areas and an immense burden on social development. Therefore, the identification of drought events and the timely determination of drought intensity could provide assistance to procedures for reducing the impacts of drought [3].

The world-recognized classification of drought has four categories: meteorological, hydrological, agricultural, and socioeconomic [4, 5]. Among these categories, the first three types are regarded to be physical phenomena. Nevertheless, drought caused by social and economic development always refers to the insufficient supply of local water [3]. Due to the increasing water demands for economic and social development, when socioeconomic drought occurs, water shortages usually affect production and consumption activities, resulting in economic, social, and environmental losses [6, 7]. It can be concluded that socioeconomic drought is most closely related to human life, but it has received the least attention [8–10]. With the expansion of industry and urbanization, in recent years, the rapid increase in water consumption has been difficult to fully satisfy with the limited water resources; thus, socioeconomic drought has gradually proven to be a serious issue requiring attention in many areas of the world [11].

Generally, the water supply of an area usually entails withdrawals from rivers. From one point of view, it can be understood that the correlation between the water intake and water demand determines the possibility of socioeconomic drought [3]. Notably, reservoirs are important

projects to manage the supply and distribution of regional water resources. The storage and discharge of a reservoir may dominate the distribution of downstream water resources, signifying that a reservoir is a system with resilience that has the ability to cope with extreme events such as floods and droughts. Therefore, the reservoir system is considered a possibility for evaluating socioeconomic drought [12].

For measuring socioeconomic drought, various kinds of indices have been developed, such as reliability, resilience, vulnerability, and integrated indices [13–17]; however, few of these indices take into account local reservoir resilience based on reservoir storage and demand [8, 10]. In this study, inspired by Mehran et al. [12], a nonparametric multivariate statistical framework to assess socioeconomic droughts was introduced for characterizing socioeconomic drought. This methodology addresses the problem that socioeconomic drought is difficult to quantify [10]. The approach is integrated by two indices, an inflow versus water demand reliability index (IDR) and a water storage resilience indicator (WSR), where the two indices are also the main characteristics of the reservoir system to cope with climate change. Then, the two indices are integrated into the proposed framework to form a new comprehensive index (i.e., multivariate standardized reliability and resilience index, MSRRI) for characterizing socioeconomic droughts.

This method provides an innovative way of evaluating socioeconomic droughts, and many scholars have utilized it to conduct related research and even made improvements to it. In Mehran et al.'s [12] paper, the indicator was used to assess socioeconomic drought during the Australian Millennium drought (1998–2010) and the 2011–2014 California drought. The results show that MSRRI is superior to univariate indices because it captures both early onset and persistence of water stress over time. Shi et al. [9] set two boundary conditions with water shortage and drought duration and proposed the socioeconomic drought index (SEDI) based on the original MSRRI. Considering the different modes of reservoir operation and management, Guo et al. [10] improved the MSRRI under the effect of reservoir operation rules. Zhao et al. [18] applied this index to Datong River Basin and compared it with historical drought events. These studies indicate that the MSRRI has a good performance in the evaluation of socioeconomic drought. However, most of these studies focused on a single reservoir, and few of them involved two or more reservoirs in watersheds despite the strong correlations. In this study, it is considered that there are spatial differences in drought conditions in the same watershed. According to the different control basin of the reservoir, each reservoir could only represent the drought situation in its own control area.

China possesses abundant rivers, and inland river basins occupy one-third of the area [8]. It is worth mentioning that the Heihe River Basin (HRB), which is the second largest inland river basin in China, has suffered from frequent water stresses and widespread desertification due to the joint impacts of climatic variations and human activities [19–21]. Two reservoirs (Huangzangsi Reservoir and Zhengyixia Reservoir) and seven hydropower stations from cascade hydropower station systems in the HRB oversee a large amount of the water and energy resources. Therefore, the HRB has long been a critical area in the arid area due to its significant role in Northwest China [8, 22, 23]. The whole basin can be divided into two regions by the two reservoirs, the up-midstream and the downstream areas. Most of the population and industries are concentrated in the up-midstream, and the downstream areas are mainly grassland and woodland. Because the water inflow downstream mainly comes from the upper and middle regions, the occurrence of drought in the lower reaches is closely related to the up-midstream. Previous studies also focused on the drought situations in the HRB, but there little attention has been paid to the correlations between the two regions.

Globally, climate variability has proven to be one of the major elements with intense teleconnections with droughts [24–26]. Advanced understanding of the spatial and temporal conjunctions between the large-scale climate indices and the variations of drought indices can enhance the science of management in water resources systems [27]. The El Niño Southern Oscillation (ENSO), which is a periodical ocean and atmospheric phenomenon, has been shown to have a strong influence on the global climate [28–32]. Many studies have verified the notable linkage between drought/flood events and extreme ENSO events existing in many parts of the world [32, 33]. In addition to ENSO, various of other studies applied the correlation analysis to evaluate the large-scale climate indices phenomena on different drought indices, such as the Pacific/North American (PNA), the North Atlantic Oscillation (NAO), Arctic Oscillation (AO), Pacific Decadal Oscillation (PDO), and East Asian summer monsoon (EASM) et al. [27, 34–39]. Besides, the utilization of spectral-based methods such as cross wavelet transform technique could improve the latent associations between a pair of time series [40]. The cross wavelet transform technique breaks down data into time and frequency space and detects the dominant variability and associated variation, which is robust in nonstationary signals [27, 41]. Considering the studies related to teleconnection indices with droughts in China, accordingly, the impacts of four large-scale climate signals (ENSO/PNA/NAO/EASM) on socioeconomic drought are examined in the present study with cross wavelet transform method.

Hence, this study takes the Heihe River Basin (HRB) in northwestern China, which is controlled by two large reservoirs, as a case study for research. The purposes of this study are as follows: (1) utilizing the MSRRI multivariate drought index to characterize the socioeconomic drought in two main reservoirs in the up-midstream and downstream regions of the HRB, respectively, and explore the relationship and differentiation of drought events between the two reaches; (2) analyzing the characteristics of the variations in socioeconomic droughts in the HRB in terms of the trends and periodicity; and (3) revealing the teleconnections between anomalous atmospheric circulation patterns (ENSO/PNA/NAO/EASM) and socioeconomic drought in the HRB.

2. Study Area and Data

Located in the central part of Eurasia, the Heihe River Basin (HRB) is the second largest inland river watershed in northwestern China. The scope of the HRB ranges from 96°E~102°E to 37.5°N~42.4°N, with a total length of 928 km and a watershed area of 128,700 km^2. Affected by human activities and climatic variations, the distribution of water resources in the HRB is extremely uneven, and population and human activities are mainly concentrated in the up-midstream area. With typical drought characteristics, the entire region of the HRB has an average annual precipitation of approximately 400 mm and an average annual potential evaporation of approximately 1,600 mm [42]. Drought has become the main cause of social development restriction and ecological environment deterioration in this area.

To solve the long-standing drought and ecological issues in the basin, two reservoirs, the Huangzangsi Reservoir and Zhengyixia Reservoir, were constructed in the HRB (Figure 1). Located in the upstream area, the Huangzangsi Reservoir is a within-year reservoir that dominates with4.06×10^8 m^3 total storage and 3.34×10^8 m^3 regulating storage, as well as 6,020 kW guaranteed output and 49,000 kW installed capacity. The Zhengyixia Reservoir is the main reservoir downstream, with a total reservoir capacity of 4.6×10^8 m^3, which has the main task of allocating the water demands for the ecosystems downstream. As these reservoirs regulate extensive water and energy resources, they will play a leading role in water resource scheduling and management in the HRB when the reservoirs are completed in 2020. Since the reservoirs have not yet been completed, only measured data of the inflow process can be accessed, and simulations of the outflow processes from July 1958 to June 2014 [43] are adopted in this study. The simulated outflow process results are verified to meet the design requirements of the reservoir. The details could be referred to [43].

Furthermore, the time series of the monthly Niño 3.4 index covering 1958~2014 was adopted to characterize ENSO events in this study, and the data were obtained from the NOAA Earth System Research Laboratory (http://www.esrl.noaa.gov/psd/data/correlation/nina34.data). The monthly PNA/NAO/EASM time series were available on the NCEP Climate Prediction Centre web page (http://www.ncdc.noaa.gov/teleconnections/ao.php). The historical data of drought records could be accessed by the China Meteorological Data Service Centre (http://data.cma.cn/).

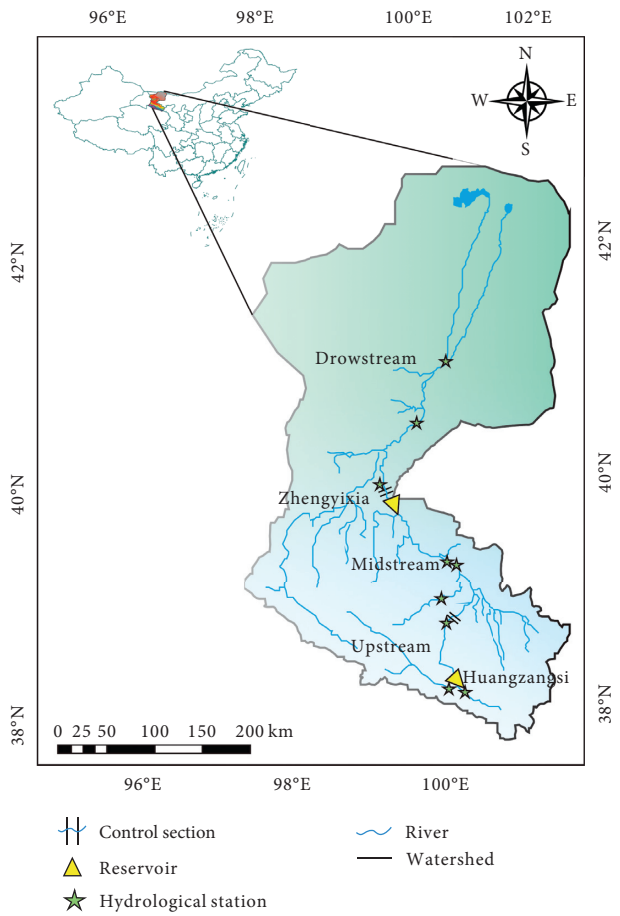

Figure 1: The location of the HRB and the reservoirs distribution.

3. Materials and Methods

3.1. The Multivariate Standardized Reliability and Resilience Index of Socioeconomic Drought. The multivariate drought index of MSRRI, as previously mentioned, consists of two individual indices, the inflow-demand reliability (IDR) and the water storage resilience (WSR) [15]. Usually, according to the regulation performance of reservoirs, reservoirs can be divided into two types: within-year and over-year reservoirs [44]. Within-year reservoirs are more sensitive to seasonality, while over-year reservoirs are more sensitive to long-term water deficiency, i.e., drought. This classification indicates that the time period has an effect on reservoir operation. With this idea, a framework was developed with the definitions for the reservoir systems being 6 months or 12 months for within-year or over-year reservoirs, respectively.

Then, two indices are defined under the frame: the IDR index and WSR index. On behalf of the available inflow, the IDR indicates if there are sufficient available water resources to satisfy the water demands for human life, regardless of the reservoir storage. Consequently, the IDR is derived by calculating the sum of the percent variation in inflow with respect to the water requirements in the predetermined time frame:

$$\alpha_t = \frac{\sum_{i=t-m+1}^{t} Q_{\text{in}_t} - Q_{\text{est}_t}}{Q_{\text{est}_t}}, \quad Q_{\text{est}_t} = \begin{cases} \sum_{i=t-12}^{t-13+m} (Q_{\text{out}})_i, & \text{if} \quad m = 6, \\ \sum_{i=t-m+1}^{t} (Q_{\text{out}})_i, & \text{if} \quad m = 12, \end{cases} \tag{1}$$

where Q_{in_i} and Q_{est_t} represent the monthly inflow of the reservoir and the total estimated water demand, respectively, and $i = 1, \ldots, N; t = 13, \ldots, N$.

Then, the WSR is calculated based on inflow, storage, and water demand at monthly timescales. Correspondingly, it is determined by whether the reservoir storages could fulfil the water demand within the time frame (m):

$$\beta_t = \frac{St_t + Q_{\text{in}_t} - Q_{\text{out}_t} - Q_{\min} - Q_{\text{est}_t}}{Q_{\text{est}_t}}, \tag{2}$$

where St_t is the reservoir storage at month t and Q_{in_i} and Q_{out_t} represent the monthly inflow of the monthly water demand. Then, $Q_{\min}$ denotes the smallest reservoir storage.

For the convenience of comparison, the standardization of the two indices with the standard normal distribution is carried out [12]. The marginal probabilities $p(x_t)$ are calculated by

$$p(x_t) = \frac{i - 0.44}{n + 0.12}, \tag{3}$$

where i represents the nonzero index ranking from small to large and n is the sample size.

Then, $p(x_t)$ is converted to a standardization index as follows. The same method is used to obtain the IDR index $\text{SI}(\alpha_t)$ and WSR index $\text{SI}(\beta_t)$.

$$\text{SI}(x) = \phi^{-1}(p). \tag{4}$$

Hence, the integration index is generated within a multivariate framework based on the Gringorten plotting position [45–47]:

$$P_{jt} = \Pr\left(\text{SI}(\alpha) \le \text{SI}(\alpha_t), \text{SI}(\beta) \le \text{SI}(\beta_t)\right),$$

$$P_{jt}\left(\text{SI}(\alpha_t), \text{SI}(\beta_t)\right) = \frac{I - 0.44}{N + 0.12}, \tag{5}$$

where P_{jt} is the joint empirical probability at month t, I represents the number of occurrences of the pair $(\text{SI}(\alpha_t), \text{SI}(\beta_t))$ for $\text{SI}(\alpha) \le \text{SI}(\alpha_t)$ and $\text{SI}(\beta) \le \text{SI}(\beta_t)$, and N is the size of the sample.

The MSRRI is formulated by the standardized joint distribution function of the IDR index $\text{SI}(\alpha_t)$ and WSR index $\text{SI}(\beta_t)$ [46]:

$$\text{MSRRI} = \phi^{-1}\left(p_j\right). \tag{6}$$

The MSRRI is an integration index relying on fundamental indices that could be utilized to estimate socioeconomic drought by measuring the supply and water storage amount related to demand. Similar to the other drought indices, this index is based on the positive and negative values to determine whether drought occurs.

The occurrence of drought events and the severity of drought need to be judged by establishing criteria. In addition to the positive and negative index values, however, because of the resiliency of the reservoir's water storage capacity, some negative values have little effect on the running process of the system. In this study, −0.8 indicates that the cumulative probability of the joint distribution of the IDR and WSR series is 0.2 and was adopted as a threshold to be the condition for drought occurrence in multivariate drought analysis [10, 46, 48, 49].

Simultaneously, the duration of drought is also an important feature for judging drought. According to the duration of drought, four grades are also established (Table 1).

Additionally, drought intensity is also an important drought characteristic. The definition of drought intensity (DI) is based on the percent of the total drought index value ($\sum VI$) to the months of drought duration (M_d) [8, 10], as shown by the following formula:

$$\text{DI} = \frac{\sum VI}{M_d}. \tag{7}$$

Consequently, for each detected socioeconomic drought event, the drought level (SDL) is defined with the indicator value V_g and duration grades D_g:

$$\text{SDL} = \max\left[V_g, D_g\right]. \tag{8}$$

3.2. The Modified Mann-Kendall (MMK) Trend Test. To analyze the features of tendency, the modified Mann-Kendall (MMK) test is adopted to examine the trends of the socioeconomic drought index series. Commonly, the Mann-Kendall (MK) method is the most widely used nonparametric method for time series trend analysis [50]. However, MK results are easily influenced by the consistency of the time series. Afterwards, the MMK trend test method, which is more robust for detecting the tendency of hydrometeorological series, was proposed [51]. Hence, this study adopted the MMK trend test method to detect the tendency of the socioeconomic drought index series.

3.3. Moving-Window Correlation Analysis (MWCA) for Periodic Component Recognition. Periodic component analysis is of great significance for understanding various hydrologic processes and predicting the future hydrological regime of a watershed or region. The moving-window correlation analysis (MWCA) proposed by Xie et al. [52] adopts a new way to test the significance of period for hydrologic series. MWCA constructs the periodic processes through correlation analysis of periodic processes and original series. To analyze the time-frequency characteristics of hydrologic series, the time-frequency centre (TFC) is also proposed to investigate the local time and frequency domain of the time series. It has been proven that MWCA exhibits good performance in identifying true periods, extracting reliable periodic components, and detecting the active time ranges of various periodic components. Therefore, MWCA is chosen to conduct the periodic analysis of socioeconomic drought series in HRB. The specific procedures could be referred to Xie et al. [52] for details.

3.4. The Cross Wavelet Analysis for Impacts of Climate Variations. Wavelet analysis has been widely used in hydrology, meteorology, and other disciplines in recent years because of its good time-frequency localization characteristics

Table 1: The classification of socioeconomic drought levels.

SDL	Definition	Intensity	Duration (months)
I	Slight	[0, 0.4]	1~6
II	Moderate	[0.4, 0.8]	6~12
III	Severe	[0.8, 1.2]	12~24
IV	Extreme	>1.2	>24

and multiresolution analysis performance. However, wavelet analysis can only explore the time-frequency characteristics of a single time series, and it is difficult to analyze the interaction and time-frequency correlation between multiple time elements. Cross wavelet transform is a new multisignal multiscale analysis technique developed on the basis of traditional wavelet analysis. This technique can not only effectively analyze the correlation degree between two associated time series but also reflect the phase structure and detailed characteristics of both time and frequency domains [53, 54].

Assuming that the background power spectra of two time series X and Y are Fourier red noise spectra P_k^X and P_k^Y, the theoretical power spectrum distribution of the cross wavelet can be expressed as [54]

$$D\left(\frac{W_n^X(s)W_n^{Y*}(s)}{\sigma_X\sigma_Y} < p\right) = \frac{Z_\nu(p)}{\nu}\sqrt{P_k^Y P_k^Y}, \quad (9)$$

where σ_X and σ_Y are the standard deviations of time series X and Y, respectively; $Z_\nu(p)$ is the confidence level associated with the probability p; and ν is degree of freedom.

For two hydrological time series X and Y, the upper 95% confidence limit of the power spectrum of red noise is obtained first. When equation (9) exceeds the confidence limit, it is considered that the results have passed the test of the standard spectrum of red noise under the condition of significance level $\alpha = 0.05$, and a significant correlation exists. The relevant codes can be freely downloaded from the website http://www.pol.ac.uk/home/research/waveletcoherence/.

Drought events are irregular in time and space in terms of distribution and severity. Some meteorological factors, such as ENSO, PNA, NAO, and EASM, are associated with drought variability. Consequently, this study explored the relevance between the MSRRI and ENSO/PNA/NAO/EASM to reveal the influences of climate indices on the socioeconomic drought in the HRB basin, which is expected to be helpful for the mitigation of local natural hazards.

4. Results and Discussions

4.1. The Evolution Characteristics of Socioeconomic Droughts in the HRB. The cascade reservoir hydropower station system in the HRB consists of two reservoirs (Huangzangsi and Zhengyixia Reservoirs) and seven hydropower stations. Therefore, the characteristics of the indicators of the two reservoirs could indicate the socioeconomic drought state of the up-middle and downstream regions of the HRB. The two reservoir systems both belong to the within-year system because they take one year to fill. Then, the time frame for them is set as 6 months.

The IDR and WSR values represent the hydrological characteristics and reservoir conditions, respectively, both relative to the demand [12]. For specifics, IDR<0 signifies a low-inflow occurrence (i.e., hydrological drought) relative to water demand, whilst WSR>0 represents the reservoir storage is sufficient for demand. Therefore, there is a phenomenon that hydrological indicators symbolize the occurrence of a drought, but the demand is satisfied by available storage, indicating that a hydrological drought may not cause a socioeconomic drought [18]. In contrary, when IDR>0 and WSR<0, it corresponds to a situation in which there is no hydrological drought based on input to reservoirs, while the system is still suffering from a socioeconomic drought as the available storage cannot meet the demand.

As integration of IDR and WSR, the MSRRI implies the synthetic information of the overall system. From Figure 2, the three lines of IDR, WSR, and MSRRI series are roughly consistent. The Pearson correlation coefficients of the monthly MSRRI series in 1958~2014 with the corresponding IDR and WSR series are 0.73 and 0.79 for Huangzangsi reservoir, respectively, as well as 0.82 and 0.88 for Zhengyixia reservoir, which indicates the reliability and effectiveness of the MSRRI in characterizing socioeconomic droughts. As integration of IDR and WSR, the smaller the MSRRI, the more severe the drought and the more serious the water shortage. The performance of the MSRRI (including IDR and WSR) applied to reservoirs is shown in Figures 2 and 3.

Overall, the MSRRI of the Huangzangsi Reservoir is lower than that of the Zhengyixia Reservoir; that is to say, the socioeconomic drought in the up-middle reaches is more serious than that in the lower reaches. There are four combinations of drought events in the upper and lower reaches: "drought occurs in both reaches," "drought occurs in only the up-midstream," "drought occurs in only the downstream," and "no drought occurs in both reaches." On a monthly scale, the probability of socioeconomic drought events occurring in the upper-middle reaches is the highest, approximately 59.8%. When drought occurs in both reaches, the drought severity in the up-midstream is greater than that in downstream (rate of 65.6%). This result confirms that the drought severity in the up-midstream is more serious than that in the downstream.

The time period of drought events (1973~1983) is selected for detailed analysis. According to the historical drought records of China Meteorological Data Service Centre, the HRB basin experienced serious drought or extreme drought in 1973, 1979~1980, 1982, and 1984, respectively. It could be seen from Figure 3 that the drought records during this period have been detected, which shows that MSRRI is applicable to the evaluation of socioeconomic droughts in HRB. The occurrence of socioeconomic drought time in the lower reaches often lags behind to a certain extent. In 1973, for example, the occurrence of drought events in the lower reaches was delayed, while the severity was higher than that in the up-middle reaches. Similarly, in approximately 1975, 1978–1980, and 1983, the downstream also experienced a lag. It can be inferred that, since the downstream mainly relies on the inflow of water from the

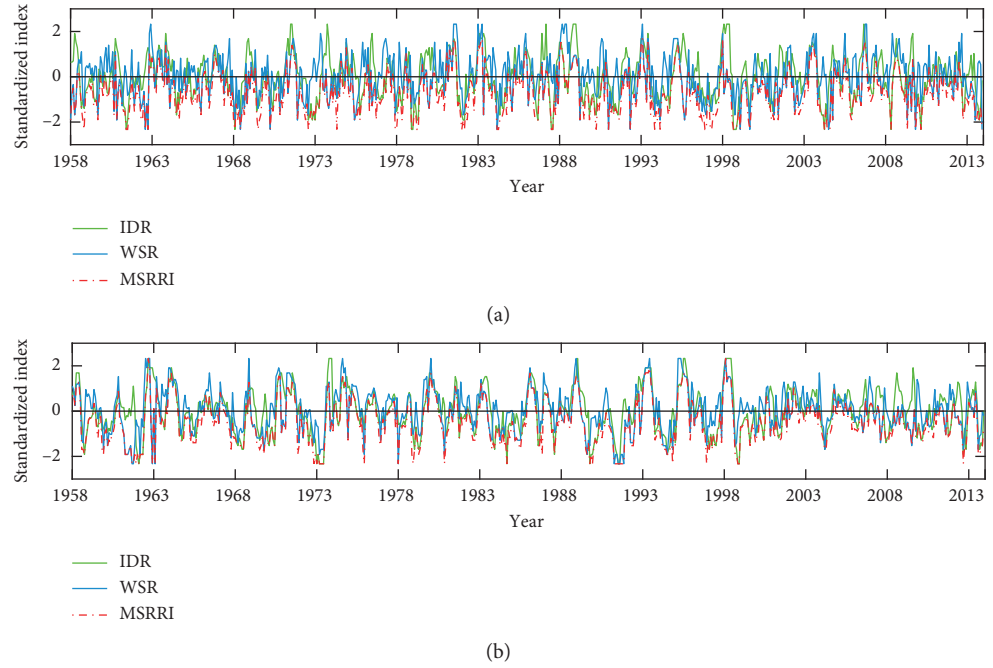

Figure 2: The monthly MSRRI series in 1958~2014 for the (a) Huangzangsi and (b) Zhengyixia Reservoirs in the HRB.

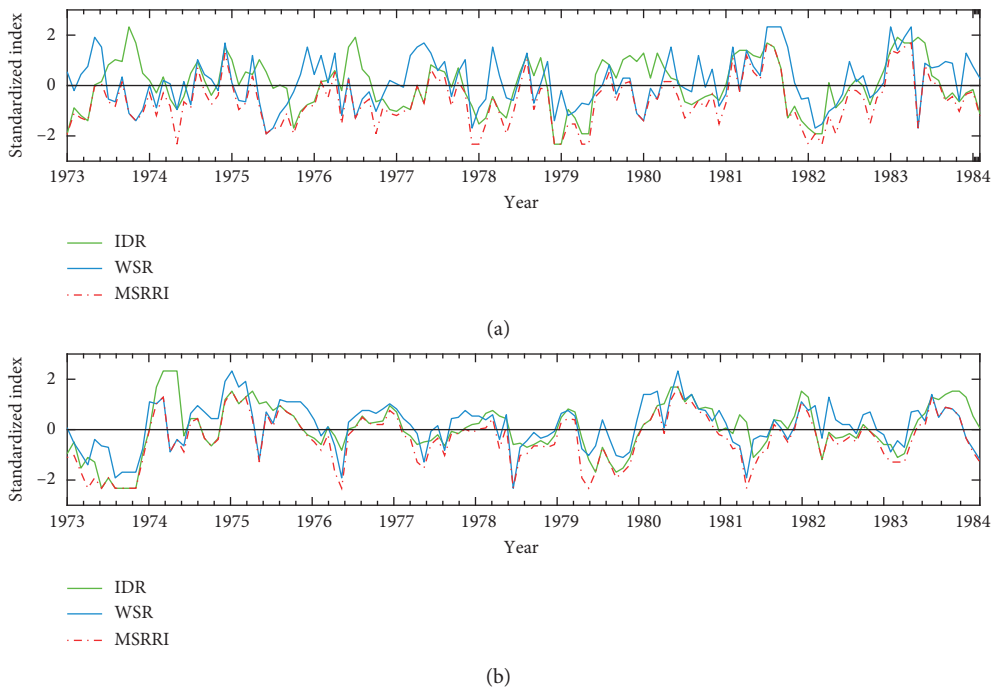

Figure 3: The specific display of the monthly MSRRI series in 1973–1983 for the (a) Huangzangsi and (b) Zhengyixia Reservoirs in the HRB.

up-midstream, when the up-midstream suffers from socioeconomic drought, the downstream of the HRB may also suffer from the resulting socioeconomic drought.

The duration and intensity of drought are usually the main characteristics of drought events. Therefore, the intensity and duration of drought are used as the basis for the comprehensive classification of socioeconomic drought in this study. The specific classification criteria are shown in Table 1 above, and the statistical results are shown in Figure 4.

It can be inferred from Figure 4 that there are distinct differences between the socioeconomic drought events in the

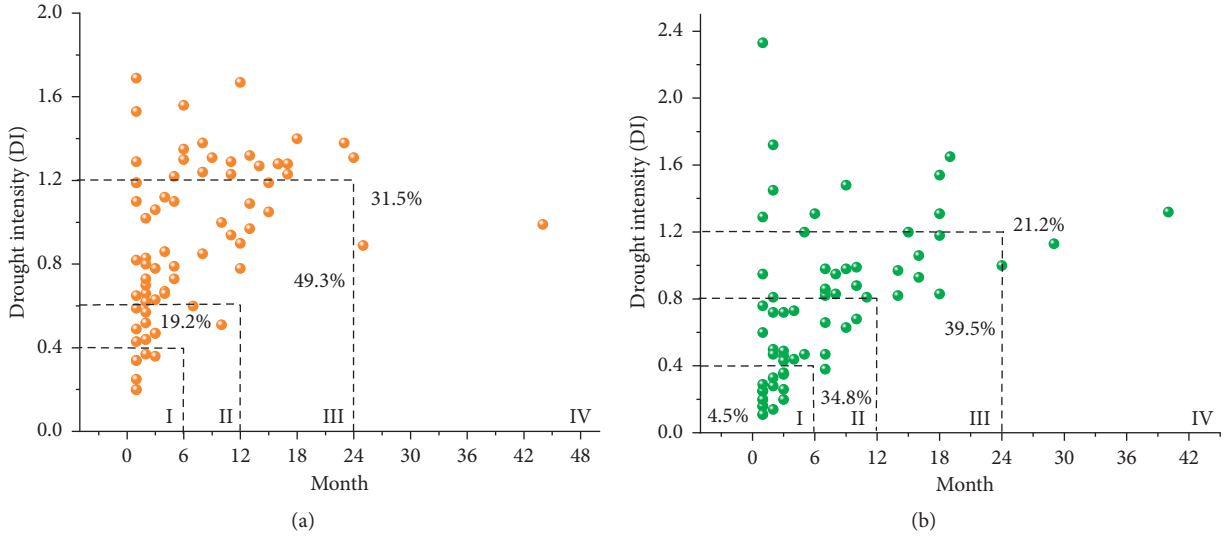

Figure 4: The statistical distribution of socioeconomic drought degrees during 1958~2014.

up-midstream and those in the downstream based on the calculation of the operation processes of the two reservoirs. This result is mainly reflected in the relatively high intensity of socioeconomic drought in the up-middle reaches. The statistical analysis of intensity and duration showed that more than 80% of the drought events in the up-middle reaches were classified as grades III or IV (49.3% and 31.5%, respectively) and that value in the downstream reaches was 60.7% (Figure 4). The number of drought events lasting for more than 12 months in the two areas was 15 and 11, respectively. Specifically, for both streams, only one drought event lasted longer than 36 months, and two drought events lasted longer than 24 months. From this point of view, the distribution of long-duration drought events in the up-middle and lower reaches is consistent. In conclusion, consistent with the above monthly MSRRI sequence analysis, the severity of socioeconomic drought in the up-midstream is higher than that in the downstream. It is necessary to be vigilant against socioeconomic drought in both the up-midstream and downstream regions due to the high risk; in particular, in the case of drought in the up-midstream, measures shall be taken in advance in the downstream.

4.2. The Trends of Socioeconomic Drought of MSRRI in the HRB. The tendency analysis in this study was carried out by the MMK trend test method of the annual and monthly MSRRI in 1958~2014 in the HRB. The results are shown in Figure 5 and Table 2.

Obviously, the MSRRI series of the two reservoirs show a growing trend on both annual and monthly scales. Among them, only the annual MSRRI of the Huangzangsi Reservoir shows a significant increasing tendency. Consistently, according to the annual trend line drawn, both reservoirs also exhibit an obvious growing trend. Consequently, the up-midstream and downstream regions in the HRB are consistent in the occurrence trend of socioeconomic drought. Moreover, this is a warning that the possibility of drought in the whole basin has been increasing.

4.3. The Periodic Component Analysis of Socioeconomic Drought in the HRB. This study utilized the MWCA method to carry out the periodicity analysis of the annul MSRRI series in the HRB at a 5% confidence level. The advantage of this method is that not only the true periodic components according to the period spectrum of time series could be found but also the estimated active time span of significant periods could be revealed with the TFC point distribution [52]. The MWCA method is used for multiple recognition rounds of the periodic components of the annual MSRRI in the HRB. The first round only identifies the most significant period of the original sequence, and then the most significant period of the remaining components of the last round is identified until no significant period occurs.

Figures 6 and 7 display the results of the periodicity analysis of the two series, in which the former is the time-domain coverage graph and the latter is the time-frequency centre distribution graph. In Figure 6, MWCA manifests one apparent period ($T = 2$ years) for the Huangzangsi Reservoir. The coverage ratio is 0.441. The Zhengyixia Reservoir has two periods ($T = 9$ and 11 years), with coverage ratios of 0.6176 and 0.4998. In addition, the estimated active time ranges of the significant period for the Huangzangsi Reservoir ($T = 3$ years) were concentrated in 1980–1996, while those for the Zhengyixia Reservoir ($T = 9$ and 11 years) were most concentrated in 1971–1988 and 1982–2013. Figure 7 shows the interruption of the 2-year period for the Huangzangsi Reservoir, which indicates that the waveform of the periodic component undergoes some changes over time. Relatively speaking, the periodic component of the up-midstream socioeconomic drought is relatively less significant than that of the downstream drought.

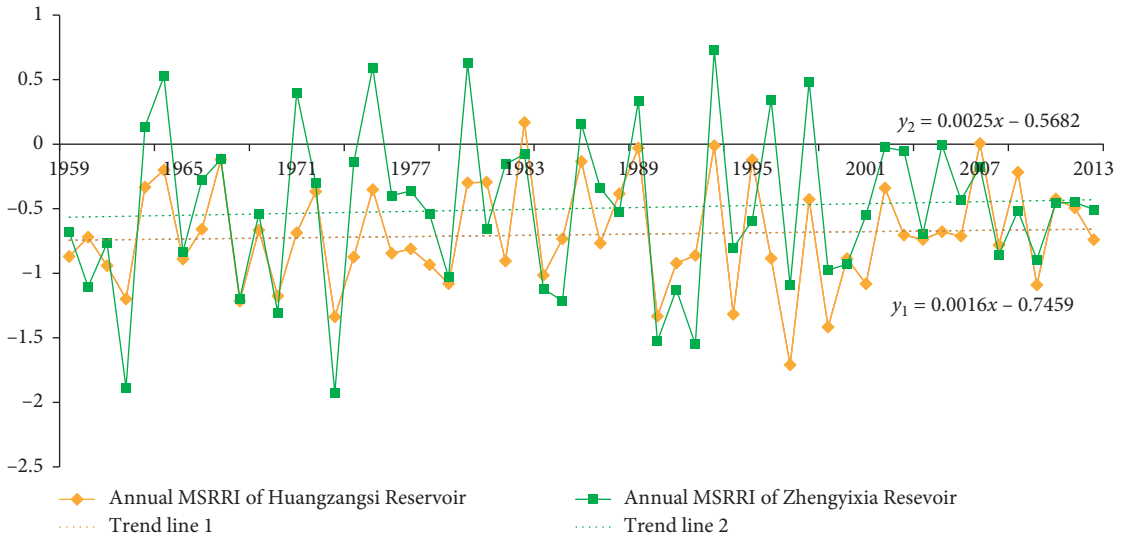

Figure 5: The annual MSRRI series for the Huangzangsi and Zhengyixia Reservoirs in 1958~2014 in the HRB.

Table 2: The MSRRI trends in 1958~2014 on monthly and annual scales in the HRB.

MMK	Sequence scale	U	α	$U\alpha/2$	Discriminant	Trend	Slope
Huangzangsi Reservoir	Annual	4.46	5%	1.96	$\|U\| > U\alpha/2$	Significant increase	0
	Monthly	0.73	5%	1.96	$\|U\| < U\alpha/2$	No significant increase	0
Zhengyixia Reservoir	Annual	0.36	5%	1.96	$\|U\| < U\alpha/2$	No significant increase	0.0027
	Monthly	1.23	5%	1.96	$\|U\| < U\alpha/2$	No significant increase	0.000188

U is the test statistics, and α is the confidence level.

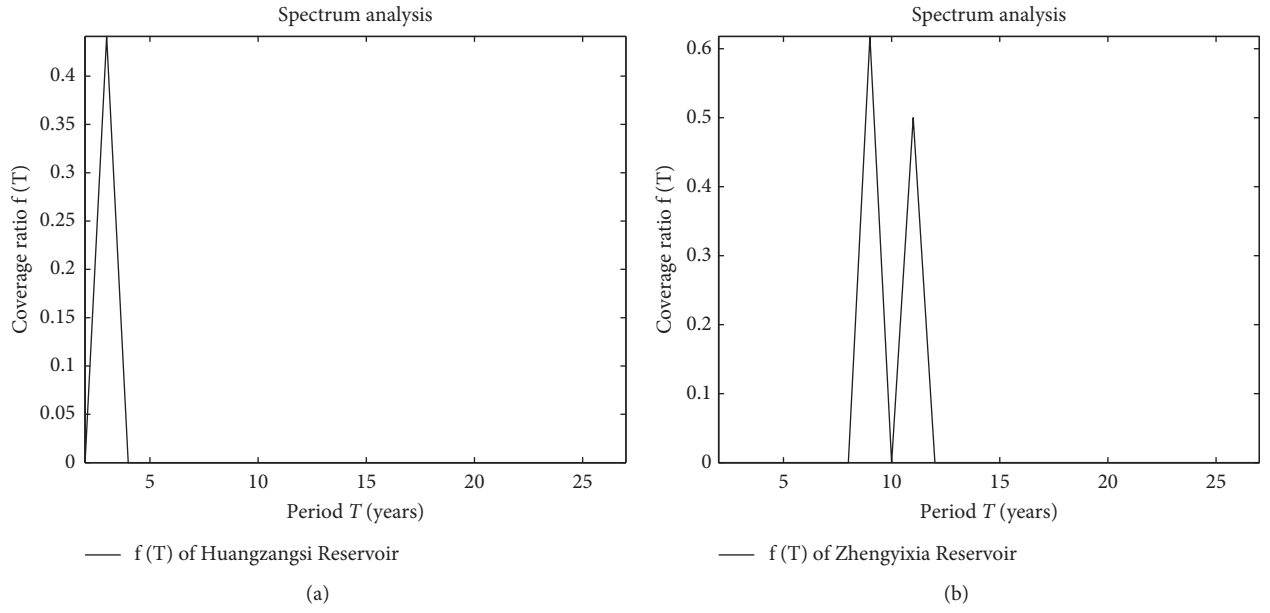

Figure 6: The periodicity analysis results of the annul MSRRI series for 1958–2014 in the HRB ((a) is for the up-midstream, and (b) is for the downstream).

4.4. The Correlations between Socioeconomic Drought and Atmospheric Circulation Factors. The linkages of socioeconomic drought with climate variability in the HRB were explored with cross wavelet analysis, and their cross wavelet transforms between the annual MSRRI series in 1958~2014 and the corresponding ENSO/PNA/NAO/EASM in the

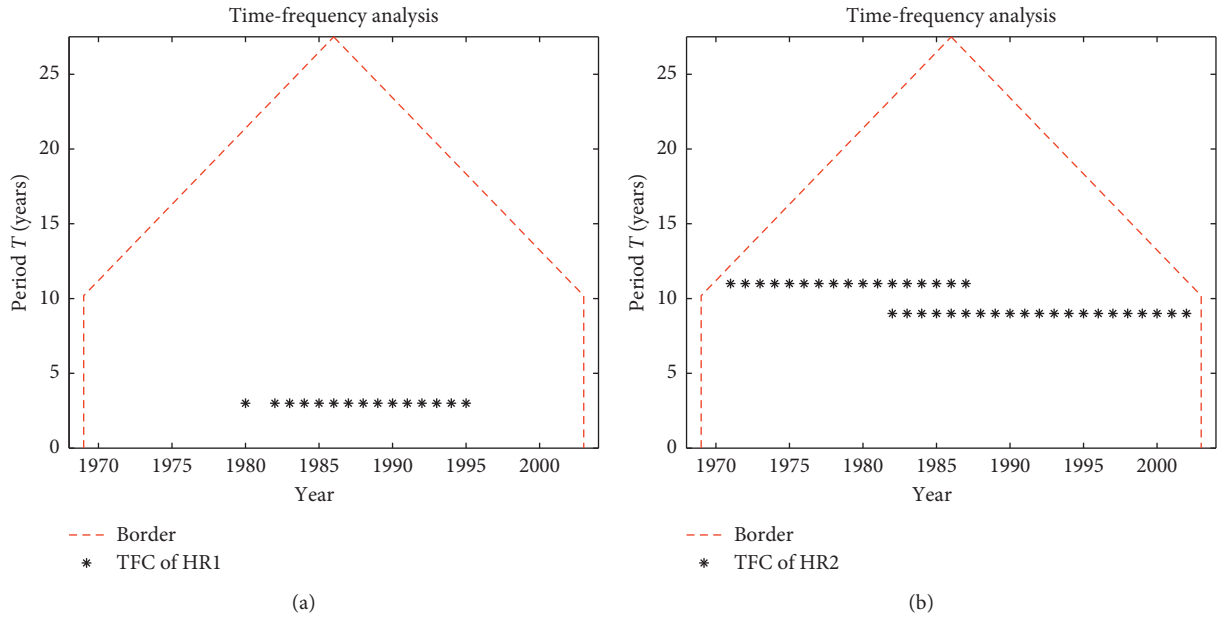

Figure 7: The results of the TFC point distribution for 1958–2014 in the HRB ((a) is for up-midstream, and (b) is for downstream).

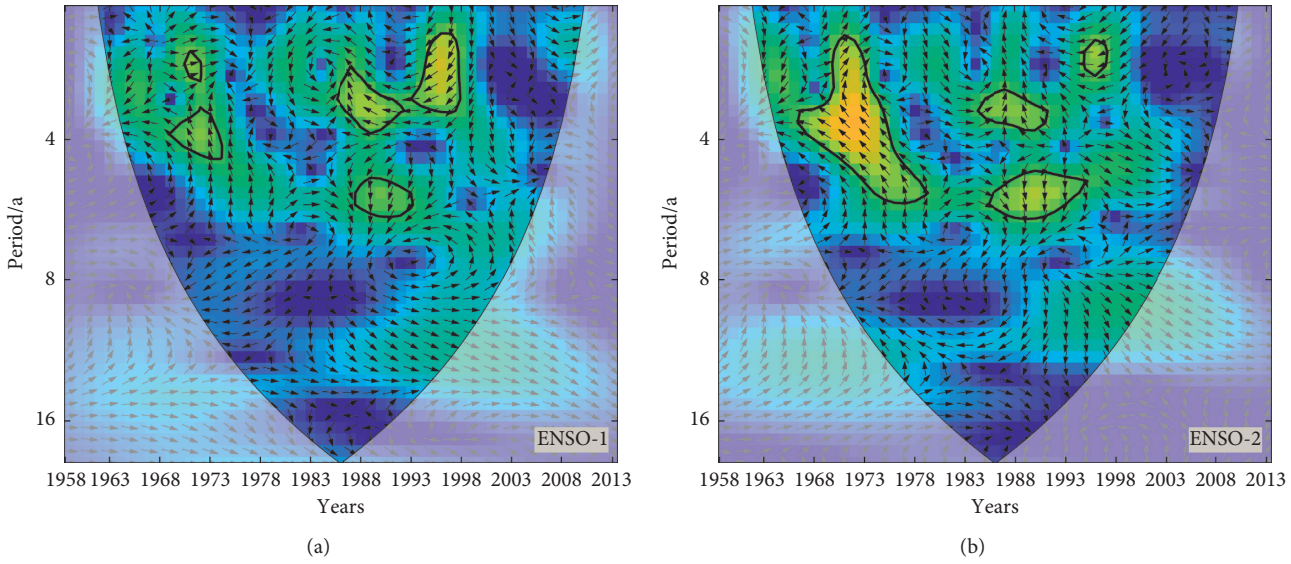

Figure 8: The cross wavelet transforms between ENSO events and annual MSRRI series in 1958~2014 in the HRB ((a) the Huangzangsi Reservoir, representing the up-midstream; (b) the Zhengyixia Reservoir, representing the downstream, the same as the following figures).

HRB are exhibited in Figures 8–11, respectively. The cross wavelet power spectrum emphasizes the correlations between drought sequence and its subsequent factors. The solid black line in the graph is the influence cone of the wavelet boundary effect, and the thick black line indicates that the domain passes the red noise test with 0.05 significance level. The relative phase relationship is represented as arrows (with anti-phase pointing left, in-phase pointing right).

Apparently, it can be seen from Figures 8–11 that these four climatic indices are more or less significantly related to the annual MSRRI series in the HRB, which indicates that the climate indices have a strong influence on the performance of socioeconomic droughts. ENSO events and the MSRRI show an inverse phase relationship; i.e., they show a strong negative phase correlation in both the up-middle and lower reaches of the region (Figure 8). In particular, the ENSO events demonstrated statistically notable negative correlations with the MSRRI series at a scale of 2~4 years in 1985~1999 in the up-midstream. For the downstream region, a significant negative linkage also exists for 2–6 years during 1969~1978. In particular, the ENSO events have a stronger influence on the downstream than on the up-midstream. Similarly, PNA also demonstrated apparent impacts on the features of socioeconomic droughts in the HRB (Figure 9). Specifically, for the upper and middle streams, PNA shows statistically notable positive linkages

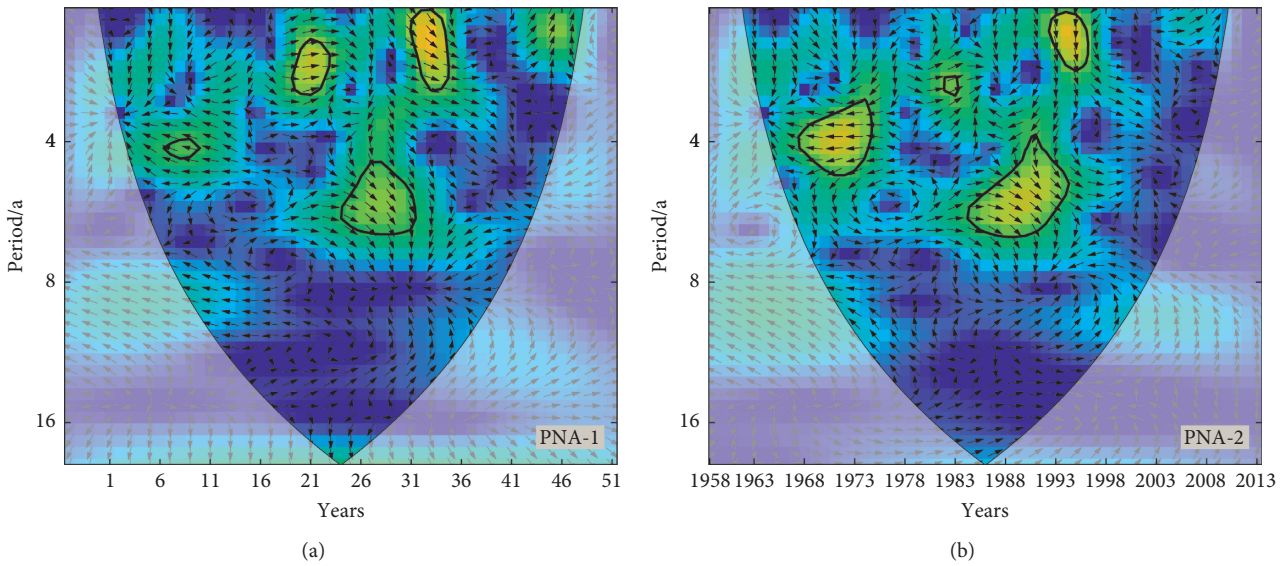

Figure 9: The cross wavelet transforms between PNA events and the annual MSRRI series in 1958~2014 in the HRB.

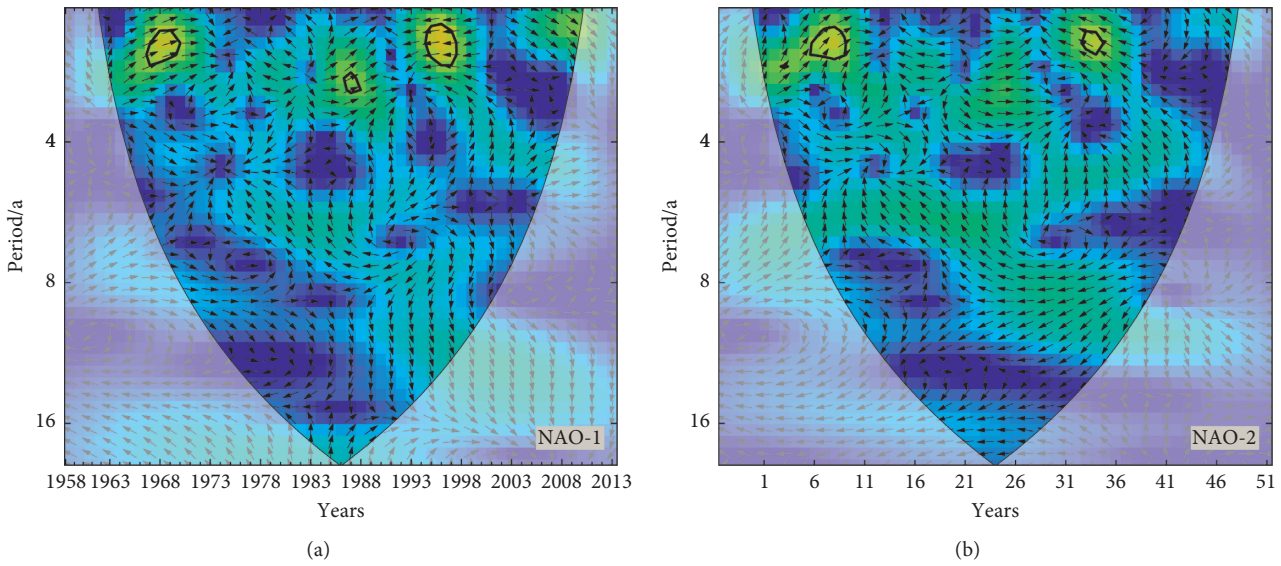

Figure 10: The cross wavelet transforms between NAO events and the annual MSRRI series in 1958~2014 in the HRB.

with the annual MSRRI series with a 2~3-year signal in 1994~1996 and a 4~6-year signal in 1988~1994. However, remarkable negative linkages exist with the annual MSRRI series with 3~5-year periods in 1967~1976. The degrees of the impact of the PNA on the socioeconomic drought events in the up-middle and lower reaches are similar. The effect of NAO on the drought of HRB basin is relatively insignificant, and the circumstances of upstream and downstream are basically consistent (Figure 10). In the whole performance period, the positive and negative positions alternate each other. For specifics, there were 2-year periodic signals with in-phase and anti-phase orientations alternately in 1968~1973 and 1993~1998, respectively. For ESAM, its impact is relatively significant and negative (Figure 11). For the up-midstream, there was a signal of about 1–4 years in 1993~1998 and a signal of about 3 years in 1978~1983. For the downstream, the signal strength is relatively obvious in 1993~1998 as the upstream with 1~2 years. In addition, there is a relatively less significant signal of 6–8 years within 1983~1993.

Overall, the comprehensive influence of the large-scale climate indices contributes to the variations in the socioeconomic droughts throughout the basin. Both positive correlations and negative correlations exist, and the periodic signals are localized. Relatively, ENSO has prominently broader and stronger impacts on socioeconomic droughts than the other teleconnection indexes. In particular, the influence of ENSO and PNA on the downstream is slightly higher than that in the up-midstream of the HRB, while the reverse is true for the NAO and EASM.

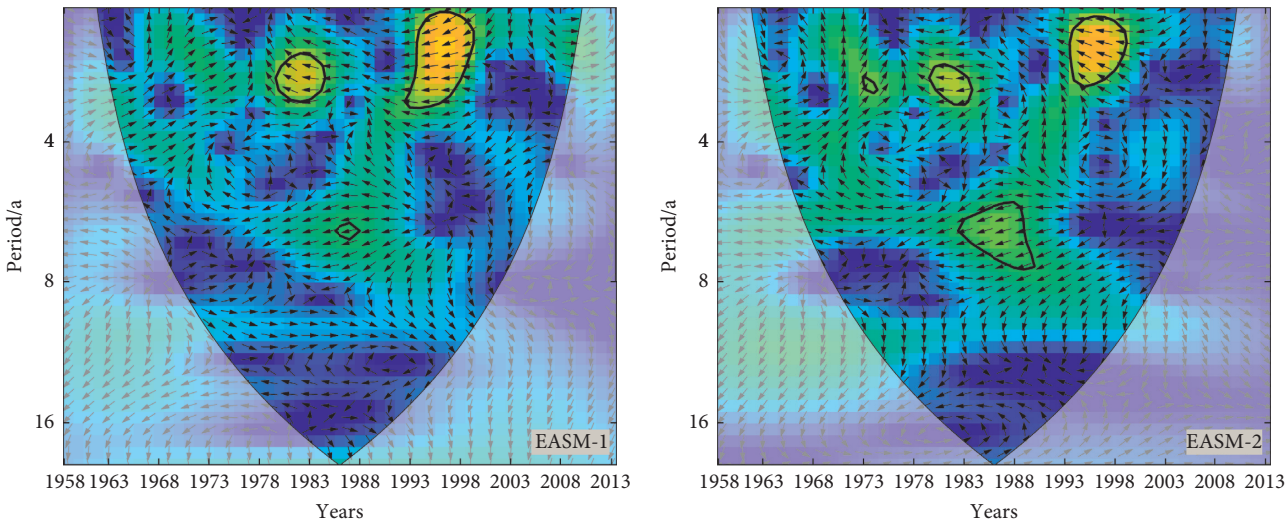

Figure 11: The cross wavelet transforms between ESAM events and the annual MSRRI series in 1958~2014 in the HRB.

5. Conclusions

As the key facility for managing regional surface water resources, reservoirs play an important role in dealing with drought and climate change. The multivariate standardized reliability and resilience index (MSRRI) is a comprehensive index for evaluating socioeconomic drought considering the water demand and water storage resilience of reservoirs. In this study, the Heihe River Basin in Northwest China, which is controlled by two large reservoirs (Huangzangsi Reservoir and Zhengyixia Reservoir) is taken as a case study, and the MSRRI is utilized to characterize the evolution features of socioeconomic drought and the linkages of large-scale climate indices.

The main results of this study showed the following:

(1) It could be inferred that the degree of socioeconomic drought in the up-midstream is higher than that in the downstream, as the rate of the annual MSRRI value in the up-mid stream, lower than that in downstream, is 65.6%. In view of the intensity and duration of drought, the statistical analysis shows that more than 80% of the drought events in the middle and upper streams are severe and extreme droughts, and only 60.7% are in the downstream, which also confirms our result. As the drought hysteresis exists in the downstream region, the occurrence of drought in the up-midstream region could be regarded as an early warning to implement preventive measures in the downstream region.

(2) An increasing trend in socioeconomic drought throughout the basin exists on both monthly and annual scales, which indicates that the increasing possibility of drought should be effectively addressed.

(3) The periodic component of the up-midstream socioeconomic drought ($T = 2$ years) is relatively less significant than that of the downstream drought. The Zhengyixia Reservoir has two periods ($T = 9$ and 11 years), with coverage ratios of 0.6176 and 0.4998.

(4) Cross wavelet analysis indicated that the large-scale climate indices contribute to the variations in the socioeconomic droughts throughout the basin, indicating that climate variability may provide a reference for managers to deal with socioeconomic drought in the HRB. Relatively, ENSO has prominently broader and stronger impacts on socioeconomic droughts than the other teleconnection indexes.

In conclusion, it is necessary for the administrative department of the Heihe River Basin to pay attention to the socioeconomic drought. This study revealed the evolution characteristics of socioeconomic drought and its relationship with climate change in the HRB, and it is expected to provide help for local socioeconomic drought resistance and water resource management.

Data Availability

The data of Nino 3.4 index used to support the findings of this study are available at the NOAA Earth System Research Laboratory (http://www.esrl.noaa.gov/psd/data/correlation/nina34.data). The data of PNA/NAO/EASM index time series used to support the findings of this study are available at the NCEP Climate Prediction Centre webpage (http://www.cpc.ncep.noaa.gov). The simulation data of outflow and storage capacity processes of reservoirs used to support the findings of this study are confidential and not accessible to the public.

Conflicts of Interest

The authors declare that there are no conflicts of interest.

Acknowledgments

The authors are very grateful to the teachers and students who have helped with this research. This study was supported by the National Natural Science Foundation of China (Grant No.51979221, 51709222), National Key R&D Program of China (Grant No. 2016YFC0401408), and Research Fund of the State Key Laboratory of Eco-hydraulics in Northwest Arid Region, Xi'an University of Technology (Grant No. 2019KJCXTD-5).

References

[1] J. Keyantash and J. A. Dracup, "The quantification of drought: an evaluation of drought indices," *Bulletin of the American Meteorological Society*, vol. 83, no. 8, pp. 1167–1180, 2002.

[2] S. Barua, A. W. M. Ng, and B. J. C. Perera, "Comparative evaluation of drought indexes: case study on the Yarra river catchment in Australia," *Journal of Water Resources Planning and Management*, vol. 137, no. 2, pp. 215–226, 2011.

[3] X. Tu, H. Wu, V. P. Singh, X. Chen, K. Lin, and Y. Xie, "Multivariate design of socioeconomic drought and impact of water reservoirs," *Journal of Hydrology*, vol. 566, pp. 192–204, 2018.

[4] D. A. Wilhite and M. H. Glantz, "Understanding: the drought phenomenon: the role of definitions," *Water International*, vol. 10, no. 3, pp. 111–120, 1985.

[5] American Meteorological Society (AMS), "Meteorological drought," *Bulletin American Meteorological Society*, vol. 85, pp. 771–773, 2003.

[6] M. Sivapalan, H. H. G. Savenije, and G. Blöschl, "Socio-hydrology: a new science of people and water," *Hydrological Processes*, vol. 26, no. 8, pp. 1270–1276, 2012.

[7] H. S. Wheater and P. Gober, "Water security and the science agenda," *Water Resources Research*, vol. 51, no. 7, pp. 5406–5424, 2015.

[8] S. Huang, Q. Huang, G. Leng, and S. Liu, "A nonparametric multivariate standardized drought index for characterizing socioeconomic drought: a case study in the Heihe River basin," *Journal of Hydrology*, vol. 542, pp. 875–883, 2016.

[9] H. Shi, J. Chen, K. Wang, and J. Niu, "A new method and a new index for identifying socioeconomic drought events under climate change: a case study of the East River basin in China," *Science of The Total Environment*, vol. 616-617, pp. 363–375, 2018.

[10] Y. Guo, S. Huang, Q. Huang et al., "Assessing socioeconomic drought based on an improved multivariate standardized reliability and resilience index," *Journal of Hydrology*, vol. 568, pp. 904–918, 2019.

[11] M. Sivapalan, "Debates-perspectives on socio-hydrology: changing water systems and the "tyranny of small problems"-socio-hydrology," *Water Resources Research*, vol. 51, no. 6, pp. 4795–4805, 2015.

[12] A. Mehran, O. Mazdiyasni, and A. AghaKouchak, "A hybrid framework for assessing socioeconomic drought: linking climate variability, local resilience, and demand," *Journal of Geophysical Research: Atmospheres*, vol. 120, no. 15, pp. 7520–7533, 2015.

[13] B. Nandintsetseg and M. Shinoda, "Assessment of drought frequency, duration, and severity and its impact on pasture production in Mongolia," *Natural Hazards*, vol. 66, no. 2, pp. 995–1008, 2013.

[14] J. F. de Oliveira-Júnior, G. de Gois, P. M. de Bodas Terassi et al., "Drought severity based on the SPI index and its relation to the ENSO and PDO climatic variability modes in the regions North and Northwest of the State of Rio de Janeiro-Brazil," *Atmospheric Research*, vol. 212, pp. 91–105, 2018.

[15] T. Hashimoto, J. R. Stedinger, and D. P. Loucks, "Reliability, resiliency, and vulnerability criteria for water resource system performance evaluation," *Water Resources Research*, vol. 18, no. 1, pp. 14–20, 1982.

[16] R. M. Vogel, M. Lane, R. S. Ravindiran, and P. Kirshen, "Storage reservoir behavior in the United States," *Journal of Water Resources Planning and Management*, vol. 125, no. 5, pp. 245–254, 1999.

[17] M. N. Ward, C. M. Brown, K. M. Baroang, and Y. H. Kaheil, "Reservoir performance and dynamic management under plausible assumptions of future climate over seasons to decades," *Climatic Change*, vol. 118, no. 2, pp. 307–320, 2013.

[18] M. Zhao, S. Huang, Q. Huang, H. Wang, G. Leng, and Y. Xie, "Assessing socio-economic drought evolution characteristics and their possible meteorological driving force," *Geomatics, Natural Hazards and Risk*, vol. 10, no. 1, pp. 1084–1101, 2019.

[19] Y. Zhang, J. Yu, P. Wang, and G. Fu, "Vegetation responses to integrated water management in the Ejina basin, northwest China," *Hydrological Processes*, vol. 25, no. 22, pp. 3448–3461, 2011.

[20] Y. Wang, Q. Feng, L. Chen, and T. Yu, "Significance and effect of ecological rehabilitation project in Inland River basins in northwest China," *Environmental Management*, vol. 52, no. 1, pp. 209–220, 2013.

[21] L. Min, J. Yu, C. Liu, J. Zhu, and P. Wang, "The spatial variability of streambed vertical hydraulic conductivity in an intermittent river, northwestern China," *Environmental Earth Sciences*, vol. 69, no. 3, pp. 873–883, 2013.

[22] S. Z. Qi and F. Luo, "Water environmental degradation of the Heihe River Basin in arid northwestern China," *Environmental Monitoring and Assessment*, vol. 108, no. 1–3, pp. 205–215, 2005.

[23] G. Cheng, X. Li, W. Zhao et al., "Integrated study of the water-ecosystem-economy in the Heihe River basin," *National Science Review*, vol. 1, no. 3, pp. 413–428, 2014.

[24] J. Aherne, T. Larssen, B. J. Cosby, and P. J. Dillon, "Climate variability and forecasting surface water recovery from acidification: modelling drought-induced sulphate release from wetlands," *Science of The Total Environment*, vol. 365, no. 1–3, pp. 186–199, 2006.

[25] R. Linares, C. Roqué, F. Gutiérrez et al., "The impact of droughts and climate change on sinkhole occurrence. A case study from the evaporite karst of the Fluvia Valley, NE Spain," *Science of the Total Environment*, vol. 579, pp. 345–358, 2017.

[26] T. Trinh, K. Ishida, M. L. Kavvas, A. Ercan, and K. Carr, "Assessment of 21st century drought conditions at Shasta Dam based on dynamically projected water supply conditions by a regional climate model coupled with a physically-based hydrology model," *Science of The Total Environment*, vol. 586, pp. 197–205, 2017.

[27] S. Vazifehkhah and E. Kahya, "Hydrological and agricultural droughts assessment in a semi-arid basin: inspecting the teleconnections of climate indices on a catchment scale," *Agricultural Water Management*, vol. 217, pp. 413–425, 2019.

[28] S. G. H. Philander, "El Niño southern oscillation phenomena," *Nature*, vol. 302, no. 5906, pp. 295–301, 1983.

[29] F. T. Cruz, G. T. Narisma, M. Q. Villafuerte, K. U. Cheng Chua, and L. M. Olaguera, "A climatological analysis of the

southwest monsoon rainfall in the Philippines," *Atmospheric Research*, vol. 122, pp. 609–616, 2013.

[30] Z. Zhang, B. F. Chao, J. Chen, and C. R. Wilson, "Terrestrial water storage anomalies of Yangtze River Basin droughts observed by GRACE and connections with ENSO," *Global and Planetary Change*, vol. 126, pp. 35–45, 2015.

[31] Z. Liu, X. Zhang, and R. Fang, "Multi-scale linkages of winter drought variability to ENSO and the Arctic Oscillation: a case study in Shaanxi, North China," *Atmospheric Research*, vol. 200, pp. 117–125, 2018.

[32] L. A. Mysak, R. G. Ingram, J. Wang, and A. Van Der Baaren, "The anomalous sea-ice extent in Hudson bay, Baffin bay and the Labrador sea during three simultaneous NAO and ENSO episodes," *Atmosphere-Ocean*, vol. 34, no. 2, pp. 313–343, 1996.

[33] V. W. Keener, G. W. Feyereisen, U. Lall, J. W. Jones, D. D. Bosch, and R. Lowrance, "El-Niño/Southern Oscillation (ENSO) influences on monthly NO3 load and concentration, stream flow and precipitation in the Little River Watershed, Tifton, Georgia (GA)," *Journal of Hydrology*, vol. 381, no. 3-4, pp. 352–363, 2010.

[34] D. J. Leathers, B. Yarnal, and M. A. Palecki, "The Pacific/North American teleconnection pattern and United States climate. Part I: regional temperature and precipitation associations," *Journal of Climate*, vol. 4, no. 5, pp. 517–528, 1991.

[35] G. J. McCabe, M. A. Palecki, and J. L. Betancourt, "Pacific and Atlantic Ocean influences on multidecadal drought frequency in the United States," *Proceedings of the National Academy of Sciences*, vol. 101, no. 12, pp. 4136–4141, 2004.

[36] H. F. Lee and D. D. Zhang, "Relationship between NAO and drought disasters in northwestern China in the last millennium," *Journal of Arid Environments*, vol. 75, no. 11, pp. 1114–1120, 2011.

[37] J. Das, S. Jha, and M. K. Goyal, "Non-stationery and copula-based approach to assess the drought characteristics encompassing climate indices over the Himalayan states in India," *Journal of Hydrology*, vol. 580, Article ID 124356, 2020.

[38] M. Xiao, Q. Zhang, V. P. Singh, and L. Liu, "Transitional properties of droughts and related impacts of climate indices in the Pearl River basin, China," *Journal of Hydrology*, vol. 534, pp. 397–406, 2016.

[39] H. Yu, T. Li, and P. Liu, "Influence of ENSO on frequency of wintertime fog days in Eastern China," *Climate Dynamics*, vol. 52, no. 9-10, pp. 5099–5113, 2019.

[40] A. Grinsted, J. C. Moore, and S. Jevrejeva, "Application of the cross wavelet transform and wavelet coherence to geophysical time series," *Nonlinear Processes in Geophysics*, vol. 11, no. 5/6, pp. 561–566, 2004.

[41] X. Tan, T. Y. Gan, and D. Shao, "Wavelet analysis of precipitation extremes over Canadian ecoregions and teleconnections to large-scale climate anomalies," *Journal of Geophysical Research: Atmospheres*, vol. 121, no. 24, pp. 14,469–14,486, 2016.

[42] J. Zhao, Z.-X. Xu, D.-P. Zuo, and X.-M. Wang, "Temporal variations of reference evapotranspiration and its sensitivity to meteorological factors in Heihe River Basin, China," *Water Science and Engineering*, vol. 8, no. 1, pp. 1–8, 2015.

[43] M. Zhao, *Research on Multi-Objective Optimal Operation of Cascade Hydropower Stations and Reservoirs in the Main Stream of Heihe River*, Xi'an University of Technology, Xi'an, China, 2019.

[44] R. M. Vogel and R. A. Bolognese, "Storage-reliability-resilience-yield relations for over-year water supply systems," *Water Resources Research*, vol. 31, no. 3, pp. 645–654, 1995.

[45] S. Yue, T. B. M. J. Ouarda, B. Bobée, P. Legendre, and P. Bruneau, "The Gumbel mixed model for flood frequency analysis," *Journal of Hydrology*, vol. 226, no. 1-2, pp. 88–100, 1999.

[46] Z. Hao and A. AghaKouchak, "A nonparametric multivariate multi-index drought monitoring framework," *Journal of Hydrometeorology*, vol. 15, no. 1, pp. 89–101, 2014.

[47] Z. Hao and V. P. Singh, "Drought characterization from a multivariate perspective: a review," *Journal of Hydrology*, vol. 527, pp. 668–678, 2015.

[48] X. Yuan, "An experimental seasonal hydrological forecasting system over the Yellow River basin-part 2: the added value from climate forecast models," *Hydrology and Earth System Sciences*, vol. 20, no. 6, pp. 2453–2466, 2016.

[49] J. Wu, C. Miao, X. Tang, Q. Duan, and X. He, "A non-parametric standardized runoff index for characterizing hydrological drought on the Loess Plateau, China," *Global and Planetary Change*, vol. 161, pp. 53–65, 2018.

[50] M. Cannarozzo, L. V. Noto, and F. Viola, "Spatial distribution of rainfall trends in Sicily (1921–2000)," *Physics and Chemistry of the Earth, Parts A/B/C*, vol. 31, no. 18, pp. 1201–1211, 2006.

[51] K. H. Hamed and A. Ramachandra Rao, "A modified Mann-Kendall trend test for autocorrelated data," *Journal of Hydrology*, vol. 204, no. 1–4, pp. 182–196, 1998.

[52] Y. Xie, Q. Huang, J. Chang, S. Liu, and Y. Wang, "Period analysis of hydrologic series through moving-window correlation analysis method," *Journal of Hydrology*, vol. 538, pp. 278–292, 2016.

[53] L. Hudgins and J. Huang, "Bivariate wavelet analysis of Asia monsoon and ENSO," *Advances in Atmospheric Sciences*, vol. 13, no. 3, pp. 299–312, 1996.

[54] C. Torrence and G. P. Compo, "A practical guide to wavelet analysis," *Bulletin of the American Meteorological Society*, vol. 79, no. 1, pp. 61–78, 1998.